Report

Current Biology

Coral-infecting parasites in cold marine ecosystems

Highlights

- Coral parasites are found in cold-water ecosystems
- They infect animals related to corals, such as anemones and corallimorphs
- Biogeography is a major factor in parasite evolution
- Current strategies for sampling microbial diversity overlook important parasites

Authors

Morelia Trznadel, Corey C. Holt, Samuel J. Livingston, Waldan K. Kwong, Patrick J. Keeling

Correspondence

pkeeling@mail.ubc.ca

In brief

Corallicolids are coral parasites that were thought to be restricted to coral reef ecosystems. Trznadel et al. show that they are widely distributed, infecting related hosts, such as anemones, in cold marine environments. This shows that corallicolids are globally relevant parasites and raises questions about biases in microbial diversity surveys.

Trznadel et al., 2024, Current Biology *34*, 1810–1816
April 22, 2024 © 2024 Elsevier Inc. All rights reserved.
https://doi.org/10.1016/j.cub.2024.03.026

CellPress

Current Biology

Report

Coral-infecting parasites in cold marine ecosystems

Morelia Trznadel,[1] Corey C. Holt,[1] Samuel J. Livingston,[1] Waldan K. Kwong,[1,2] and Patrick J. Keeling[1,3,4,*]
[1]Botany Department, University of British Columbia, 6270 University Boulevard, Vancouver, BC V6T 1Z4, Canada
[2]Present address: Instituto Gulbenkian de Ciência, Rua da Quinta Grande 6 2780-156 Oeiras, Portugal
[3]X (formerly Twitter): @pjkeelinglab
[4]Lead contact
*Correspondence: pkeeling@mail.ubc.ca
https://doi.org/10.1016/j.cub.2024.03.026

SUMMARY

Coral reefs are a biodiversity hotspot,[1,2] and the association between coral and intracellular dinoflagellates is a model for endosymbiosis.[3,4] Recently, corals and related anthozoans have also been found to harbor another kind of endosymbiont, apicomplexans called corallicolids.[5] Apicomplexans are a diverse lineage of obligate intracellular parasites[6] that include human pathogens such as the malaria parasite, *Plasmodium*.[7] Global environmental sequencing shows corallicolids are tightly associated with tropical and subtropical reef environments,[5,8,9] where they infect diverse corals across a range of depths in many reef systems, and correlate with host mortality during bleaching events.[10] All of this points to corallicolids being ecologically significant to coral reefs, but it is also possible they are even more widely distributed because most environmental sampling is biased against parasites that maintain a tight association with their hosts throughout their life cycle. We tested the global distribution of corallicolids using a more direct approach, by specifically targeting potential anthozoan host animals from cold/temperate marine waters outside the coral reef context. We found that corallicolids are in fact common in such hosts, in some cases at high frequency, and that they infect the same tissue as parasites from topical coral reefs. Parasite phylogeny suggests corallicolids move between hosts and habitats relatively frequently, but that biogeography is more conserved. Overall, these results greatly expand the range of corallicolids beyond coral reefs, suggesting they are globally distributed parasites of marine anthozoans, which also illustrates significant blind spots that result from strategies commonly used to sample microbial biodiversity.

RESULTS AND DISCUSSION

Corallicolids commonly infect cold-water anthozoan hosts

Analyses of environmental data have consistently shown corallicolids are restricted to coral reef environments.[8,9,11] Although this correlation is striking, it may be misleading because the vast majority of marine sequence data currently comes from the water column and, to a lesser extent, benthic substrates. Sampling these environments will successfully measure parasitic diversity only if the parasite broadcasts some life stages into the environment, as do, for instance, marine alveolate (MALV) dinoflagellates.[12] However, many parasites, including many apicomplexans, have comparatively closed infection strategies—moving from one host to another with only limited exposure to the outside environment—and these will escape detection without direct sampling of their hosts.[13,14] Corals attract a lot more attention than most invertebrates, so it is possible, despite the hundreds of millions of data points suggesting the opposite,[8] that the corallicolids have a much wider geographical distribution than presently appreciated. Indeed, the discovery of corallicolids in subtropical Anthozoa sampled from deep water off coral reef ecosystems[9] suggests they can survive in cold temperatures. But the only direct information on their occurrence in plausible hosts from ecosystems outside tropical or subtropical coral reef environments is a comprehensive biogeographical examination of the temperate sea anemone, *Anthopleura elegantissima*, whose bacterial microbiome yielded no indication of corallicolid plastids across the Northeast Pacific.[15] Though this is consistent with the conclusion that corallicolids are restricted to tropical and subtropical coral reefs, it is also based on a single species.

To more systematically test whether corallicolids are more widespread geographically, we collected 325 samples from nine species of cold-water anthozoans from non-coral reef environments at five locations in coastal British Columbia (BC). Collectively, this covers a diverse range of anthozoans from cold water in temperate marine environments, including stony corals, sea anemones, corallimorphs, zoanthids, octocorals, and tube-dwelling anemones (see Figure 1A for a summary of anthozoan groups). Samples were screened for corallicolid infection using PCR and sequencing of nuclear small subunit rRNA (SSU rRNA). This confirmed the lack of corallicolids in *Anthopleura elegantissima*,[15] but showed other cold-water anthozoans are in fact infected, some at high frequency. The anemone *Metridium senile* appeared to have the highest rates of infection,

 © 2024 Elsevier Inc. All rights reserved.

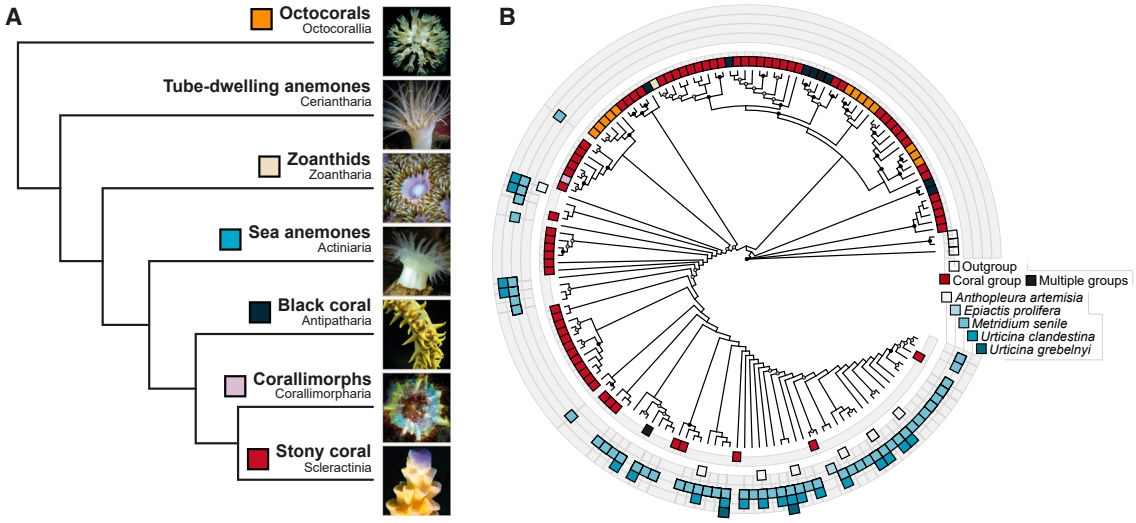

Figure 1. Corallicolids infect diverse cold-water anthozoans

(A) A schematic tree of anthozoan subgroups showing for each a picture and how the subgroups are related, as well as their formal taxonomic name and the common name used throughout this paper.

(B) Amplicon sequence variants (ASVs) representing the diversity of corallicolids in anthozoan microbiomes. The cladogram shows the relationship of ASVs in a ML phylogeny. ASVs come from publicly available microbiome data from corals (Table S1), in addition to the corallicolids from anemone microbiomes characterized in this study (see Table S2; Figure S1 for a full catalog of all eukaryotic ASVs found in the newly characterized microbiomes). Colored boxes indicate host identity using the colors for each subgroup shown in (A). All sea anemone microbiomes are from cold habitats and are shown in different shades of blue, each indicating a particular host species, as listed in the key. For all other groups, all sampling is from tropical and subtropical reef environments and a single color is used to represent any species from that group.

See also Tables S1 and S2.

with 77.8% of individuals testing positive (n = 36), followed by the corallimorph *Corynactis californica*, in which 68.7% of tested individuals were infected (n = 32). The anemones *Anthopleura artemisia* and *Urticina grebelyni* were also infected, but at lower rates (Table S1). Corallicolids were not detected or detected at very low frequencies in only a couple of individuals in *Pachycerianthus* sp. and *Urticina clandestinea,* respectively (Table S1). To corroborate these findings, deep sequencing of the eukaryotic microbiome was carried out for representative positive- and negative-testing species. This confirmed the presence of numerous genetically distinct corallicolids in a variety of cold-water anemones (Figure 1B) and suggested that even in species where infection frequency is high (e.g., *M. senile*), the parasite load within a given host is likely low (Figure S1). The bacterial microbiome was also sequenced, but sequences corresponding to corallicolid plastid SSU rRNA in BC samples were not observed, although we could detect them in anemones from tropical coral reefs. This may be because the copy number of plastid SSU is lower, as in other corallicolids,[5] or because of an amplification bias.

To directly observe the presence and frequency of cold-water corallicolids in their host, and also determine if they infect the same tissue as in tropical hosts, we examined the two hosts with the highest infection rates (the anemone *M. senile* and the corallimorph *C. californica*; Figure 2) using fluorescence *in situ* hybridization (FISH). In both hosts, the nematocysts exhibited non-specific DNA probe interaction that had to be quenched with a EUB338 universal bacterial probe pre-incubation (Figures S2D and S2E). Corallicolids were positively identified in *C. californica* mesenterial filaments with low prevalence (1–2 cell clusters per filament; Figure 2), and no infected cells were detected in 20 individuals of *M. senile* that were imaged after testing positive in molecular screening. This confirms that cold-water corallicolids can infect the same tissue as coral reef parasites,[5] and is also consistent with the molecular survey data suggesting very low parasite loads even in frequently infected cold-water hosts.

What drives the structure of corallicolid diversity?

Environmental sequences are too short to yield a well-supported phylogeny, but we nevertheless noted an obvious tendency for amplicon sequence variants (ASVs) from temperate anemone parasites to cluster together to the exclusion of parasites from coral reefs in Figure 1 (note the clustering of blue- and red-shaded boxes). Though this may at first glance appear to suggest that the temperature of the habitat is an important factor in corallicolid ecology or evolution, there are actually several possible explanations—providing that the phylogeny based on short sequence reads is even a correct representation of the data. For example, coral reef sampling is strongly biased toward stony corals and locations in the Atlantic, whereas cold-water hosts are biased toward anemones and to the Pacific. To test whether the phylogenetic separation is genuine, and to better distinguish between potential drivers behind this separation, we characterized full-length SSU rRNA genes from communities of corallicolids in *M. senile* and *C. californica*. To better address the possibility that host taxonomy was a factor, we also sampled five species of anemone from the tropical coral reef environment, identified two species of *Edwardsiella* anemones from Curaçao (Figures 2C and 2D) with high infection frequencies, and

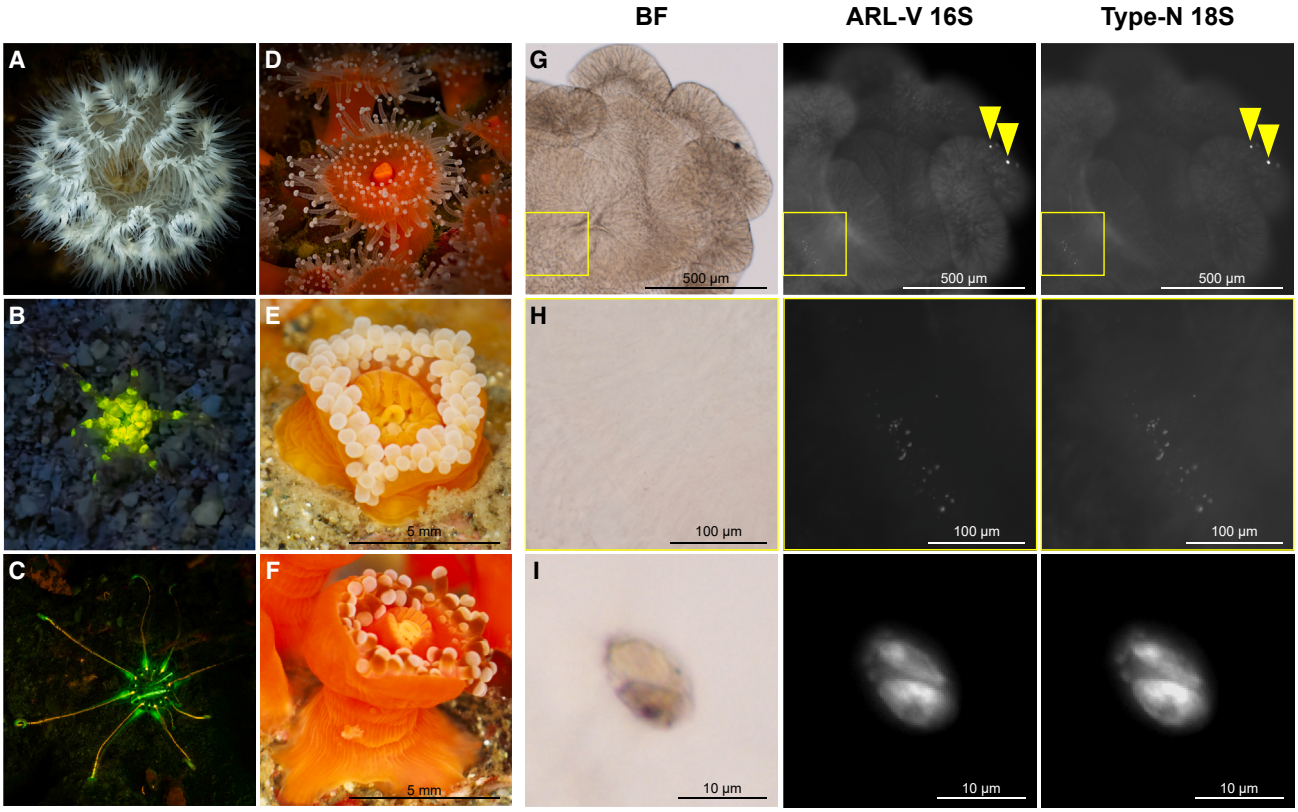

Figure 2. Cold-water corallicolids and hosts

(A–D) Host species that were chosen for detailed observations as they appear in their natural habitat: (A) the white plumose anemone, *Metridium senile*; (B) and (C) two undescribed members of the genus *Edwardsiella*, both small, transparent sand-dwelling anemones from coral reef environments (both pictured at night using blue light to excite their fluorescence, as this is how they were found and sampled in nature); and (D) the corallimorph confusingly known as the strawberry anemone, *Corynactis californica*.

(E and F) Two specific individuals of *C. californica* that tested positive for corallicolids and were analyzed by microscopy, shown to the right.

(G–I) Fluorescence *in situ* hybridization showing corallicolids in mesenterial filaments of *C. californica*. In each panel on the left is a bright-field (BF) image of fixed tissue with the same fields shown hybridized to probes for corallicolid plastid (center: ARL-V 16S) and nuclear SSU rRNA (right: Type-N 18S). See Figure S2 for controls. Each panel shows infection at different magnifications: (G) low magnification image of a whole mesenterial filament with two infection foci; (H) shows a close up of several foci in a mesenterial filament; and (I) shows a high magnification of two corallicolid cells in a membrane, which we interpret to be intracellular stages released from their host cell during fixation. All samples were pre-incubated with blocking primers to reduce non-specific hybridization to nematocysts (see Figure S2).

characterized full-length SSU rRNA genes from their corallicolid communities.

The phylogenetic tree based on these longer sequences was inferred using ML and Bayesian methods, resulting in a tree with greater resolution and statistical support, but still representing parasites sampled from various hosts, climates, depths, and geographical zones and locations (Figure 3). Not every node of the tree is supported, and no factor correlates perfectly with the phylogeny, but if we examine the most strongly supported nodes of the tree (e.g., above the 85%–90% level), it is evident that some criteria correlate with the phylogeny better than others. Host order and latitude correlate very poorly with phylogeny, except at the shallowest level in the tree; at deeper levels they are scattered among several highly supported clades. This is not to say these criteria do not impact corallicolid diversity, but rather that their effects are likely most important over short evolutionary timescales; closely related hosts may have closely related parasites, but there is no "anemone clade", and host-parasite co-evolution does not appear to be a major factor at a deep phylogenetic level. This is consistent with previous observations from the Gulf of Mexico and Caribbean, which found no strict clustering based on host species but noted associations of some corallicolids with hosts at lower taxonomic levels.[9] Water depth and latitudinal zone tended to cluster somewhat more, but sampling across these criteria is also more biased as there are relatively few samples from greater depth and higher latitudinal zones and they tend to be co-biased with location and host identity, making these promising factors for further study. The factor that currently correlates most strongly with ancient branches in the tree is geographical location. All the deepest-branching and best-supported clades in the phylogeny (e.g., every clade supported over 85%) include only samples either from the Atlantic or the Pacific Oceans. There are more weakly supported groups in both Figures 1 and 3 that include both Atlantic and Pacific samples, so parasites may spread at some low frequency; nevertheless it does seem that geography plays

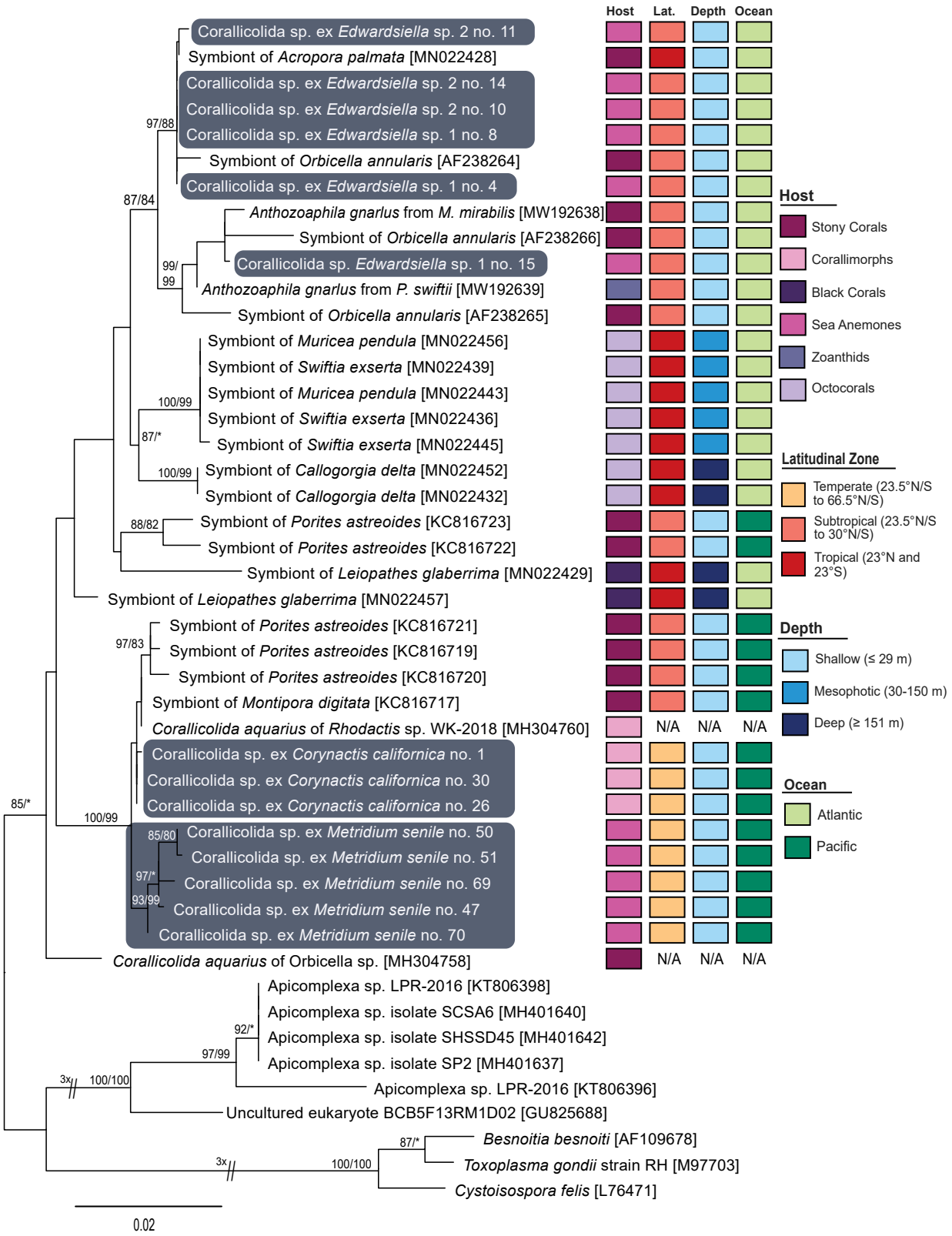

Figure 3. Biogeography and corallicolid diversity

Maximum likelihood phylogeny of all available SSU rRNA genes from corallicolids greater than 800 base pairs (bp) in length (with two exceptions being slightly shorter sequences generated in this study—Corallicolid sp. ex *Metridium senile* no. 69 and Corallicolid sp. ex *Metridium senile* no. 70; see STAR Methods and

(legend continued on next page)

major role in structuring the diversity of corallicolids over long evolutionary timescales.

These observations lead to interesting questions about parasites from other regions. For example, consider the range of *M. senile* (or something very closely related to it, as the species-level taxonomy is in flux), which extends from the North Pacific to the North Atlantic. If corallicolids infect Atlantic *M.* senile, are they more closely related to Pacific corallicolids from the same host, or alternatively more similar to tropical Atlantic corallicolids, as the phylogenetic pattern would currently suggest? Corallicolids from other areas, such as the West Pacific, Mediterranean, Red Sea, or Indian Ocean, might also help reveal larger biogeographical patterns underlying the spread of these parasites around the world's oceans.

Implications for microbial biodiversity sampling

The discovery of corallicolids in coral hosts led to them being called a "third player in the game" of coral symbiosis.[5,16] Indeed, their tight association with coral tissue, observed directly and also in the striking correlation between the presence of corallicolid sequences and coral reef environments,[5,8,11] further reinforced this. However, here we show that, despite the overwhelming signal for this correlation in environmental data, corallicolids are not restricted to tropical reef regions, but are likely globally distributed parasites of diverse anthozoans in all their marine habitats. This example has implications for the way we sample, measure, and interpret environmental diversity, because it is clearly missing an important and potentially massive fraction of that diversity. Parasites are known to be both hugely diverse and very important in structuring natural communities, including both animal and protist hosts.[12,17–20] Some of these are already appreciated to be important and major components of marine diversity. For example, marine alveolates (MALVs) are two lineages that typically account for as much as 60% of sequences in surveys of marine eukaryotic diversity,[12,19,20] and they are so well represented because they broadcast huge numbers of infectious cells into the water column as a key part of their parasitic strategy.[12,20] Our direct observations also support this (Figure S1), because MALVs were one of the most prevalent classes in the anemone microbiomes (60.5% of all samples) and showed the highest average relative abundance across all samples (21%). But we also know that other important parasitic lineages remain in a tight physical association with their host or hosts throughout their life cycle,[13,14,21,22] and indeed it appears that corallicolids likely fall into this camp.[23] The importance of these on land is well documented (e.g., consider malaria, which is abundant in many parts of the world and virtually never found outside a host), but in the ocean these continue to fly under our radar, probably because of sampling bias.[22] Indeed, corallicolids were only discovered because of an unrelated interest in the bacteria associated with coral.[11] To see this kind of diversity more clearly, we need to change the way we define "the environment" to include the bodies of animals and other potential hosts within the larger environment, because they are a reservoir of an interesting and ecologically significant component of biodiversity that is not represented anywhere else.[12,19] When we do so, we anticipate that a number of new or understudied parasitic and host-associated groups will turn out to be diverse, widespread, and ecologically significant, despite currently being totally invisible.

STAR★METHODS

Detailed methods are provided in the online version of this paper and include the following:

- KEY RESOURCES TABLE
- RESOURCES AVAILABILITY
  - Lead contact
  - Materials availability
  - Data and code availability
- EXPERIMENTAL MODEL AND STUDY PARTICIPANT DETAILS
- METHOD DETAILS
  - Screening of corallicolid infection
  - Microbiome sequencing and phylogenetic analysis
  - Full-length SSU sequencing and phylogenetic analysis
  - Fluorescence *in situ* hybridization (FISH)

SUPPLEMENTAL INFORMATION

Supplemental information can be found online at https://doi.org/10.1016/j.cub.2024.03.026.

ACKNOWLEDGMENTS

We thank Mark Vermeij at CARMABI Research Station for providing expert advice and support in the field, the UBC Bioimaging Facility (RRID: SCR_021304) for imaging support, and the many people who accompanied us on sampling trips during COVID. This work was supported by grants to P.J.K. from the Gordon and Betty Moore Foundation (https://doi.org/10.37807/GBMF9201) and Hakai Institute.

AUTHOR CONTRIBUTIONS

The study was conceived by P.J.K. and M.T., collections were done by M.T. and P.J.K., data generation by M.T. and S.J.L., data analysis done by M.T. and C.C.H., project supervision was provided by W.K.K. and P.J.K., and funding acquired by P.J.K.

DECLARATION OF INTERESTS

The authors declare no competing interests.

Received: December 6, 2023
Revised: February 17, 2024
Accepted: March 14, 2024
Published: April 11, 2024

Table S3). New lineages characterized in this study are highlighted by gray boxes. Bootstrap and posterior probability support above 80% or 0.8 are indicated at each node. To the right, four variables are indicated by color-coded boxes: host order, latitudinal zone, sampling depth, and geographical location. Clades supported at 85% or greater consistently contain sequences from the same ocean. Hosts acquired from the aquarium trade branched in a position consistent with their expected geographical origin, but because their exposure to other potential hosts since their collection cannot be ruled out, variables other than the host are left blank. Additional trees based on Bayesian analyses or with additional short sequences are available in Figure S3.
See also Table S3.

REFERENCES

1. Tittensor, D.P., Mora, C., Jetz, W., Lotze, H.K., Ricard, D., Berghe, E.V., and Worm, B. (2010). Global patterns and predictors of marine biodiversity across taxa. Nature *466*, 1098–1101. https://doi.org/10.1038/nature09329.
2. Hughes, T.P., Barnes, M.L., Bellwood, D.R., Cinner, J.E., Cumming, G.S., Jackson, J.B.C., Kleypas, J., van de Leemput, I.A., Lough, J.M., Morrison, T.H., et al. (2017). Coral reefs in the Anthropocene. Nature *546*, 82–90. https://doi.org/10.1038/nature22901.
3. Stat, M., Morris, E., and Gates, R.D. (2008). Functional diversity in coral–dinoflagellate symbiosis. Proc. Natl. Acad. Sci. USA *105*, 9256–9261. https://doi.org/10.1073/pnas.0801328105.
4. Liu, H., Stephens, T.G., González-Pech, R.A., Beltran, V.H., Lapeyre, B., Bongaerts, P., Cooke, I., Aranda, M., Bourne, D.G., Forêt, S., et al. (2018). Symbiodinium genomes reveal adaptive evolution of functions related to coral-dinoflagellate symbiosis. Commun. Biol. *1*, 95–11. https://doi.org/10.1038/s42003-018-0098-3.
5. Kwong, W.K., del Campo, J., Mathur, V., Vermeij, M.J.A., and Keeling, P.J. (2019). A widespread coral-infecting apicomplexan with chlorophyll biosynthesis genes. Nature *568*, 103–107. https://doi.org/10.1038/s41586-019-1072-z.
6. Votýpka, J., Modrý, D., Oborník, M., Šlapeta, J., and Lukeš, J. (2017). Apicomplexa. In Handbook of the Protists, J.M. Archibald, A.G.B. Simpson, C.H. Slamovits, L. Margulis, M. Melkonian, D.J. Chapman, and J.O. Corliss, eds. (Springer International Publishing), pp. 1–58. https://doi.org/10.1007/978-3-319-32669-6_20-1.
7. J.J. Lee, ed. (2000). An illustrated guide to the Protozoa, 1 2nd. ed. (The Society for Protozoology).
8. Mathur, V., del Campo, J., Kolisko, M., and Keeling, P.J. (2018). Global diversity and distribution of close relatives of apicomplexan parasites. Environ. Microbiol. *20*, 2824–2833. https://doi.org/10.1111/1462-2920.14134.
9. Vohsen, S.A., Anderson, K.E., Gade, A.M., Gruber-Vodicka, H.R., Dannenberg, R.P., Osman, E.O., Dubilier, N., Fisher, C.R., and Baums, I.B. (2020). Deep-sea corals provide new insight into the ecology, evolution, and the role of plastids in widespread apicomplexan symbionts of anthozoans. Microbiome *8*, 34. https://doi.org/10.1186/s40168-020-00798-w.
10. Bonacolta, A.M., Miravall, J., Gómez-Gras, D., Ledoux, J.-B., López-Sendino, P., Garrabou, J., Massana, R., and Campo, J. del (2023). Apicomplexans predict thermal stress mortality in the Mediterranean coral Paramuricea clavata. Preprint at bioRxiv. https://doi.org/10.1101/2022.11.23.517658.
11. Janouškovec, J., Horák, A., Barott, K.L., Rohwer, F.L., and Keeling, P.J. (2012). Global analysis of plastid diversity reveals apicomplexan-related lineages in coral reefs. Curr. Biol. *22*, R518–R519. https://doi.org/10.1016/j.cub.2012.04.047.
12. Holt, C.C., Hehenberger, E., Tikhonenkov, D.V., Jacko-Reynolds, V.K.L., Okamoto, N., Cooney, E.C., Irwin, N.A.T., and Keeling, P.J. (2023). Multiple parallel origins of parasitic Marine Alveolates. Nat. Commun. *14*, 7049. https://doi.org/10.1038/s41467-023-42807-0.
13. Meibalan, E., and Marti, M. (2017). Biology of Malaria Transmission. Cold Spring Harb. Perspect. Med. *7*, a025452. https://doi.org/10.1101/cshperspect.a025452.
14. Jalovecka, M., Sojka, D., Ascencio, M., and Schnittger, L. (2019). Babesia Life Cycle – When Phylogeny Meets Biology. Trends Parasitol. *35*, 356–368. https://doi.org/10.1016/j.pt.2019.01.007.
15. Morelan, I.A., Gaulke, C.A., Sharpton, T.J., Vega Thurber, R., and Denver, D.R. (2019). Microbiome Variation in an Intertidal Sea Anemone Across Latitudes and Symbiotic States. Front. Mar. Sci. *6*.
16. Richards, T.A., and McCutcheon, J.P. (2019). Coral symbiosis is a three-player game. Nature *568*, 41–42. https://doi.org/10.1038/d41586-019-00949-6.
17. Morrison, D.A. (2009). Evolution of the Apicomplexa: where are we now? Trends Parasitol. *25*, 375–382. https://doi.org/10.1016/j.pt.2009.05.010.
18. Worden, A.Z., Follows, M.J., Giovannoni, S.J., Wilken, S., Zimmerman, A.E., and Keeling, P.J. (2015). Rethinking the marine carbon cycle: Factoring in the multifarious lifestyles of microbes. Science *347*, 1257594. https://doi.org/10.1126/science.1257594.
19. de Vargas, C., Audic, S., Henry, N., Decelle, J., Mahé, F., Logares, R., Lara, E., Berney, C., Le Bescot, N., Probert, I., et al. (2015). Eukaryotic plankton diversity in the sunlit ocean. Science *348*, 1261605. https://doi.org/10.1126/science.1261605.
20. Guillou, L., Viprey, M., Chambouvet, A., Welsh, R.M., Kirkham, A.R., Massana, R., Scanlan, D.J., and Worden, A.Z. (2008). Widespread occurrence and genetic diversity of marine parasitoids belonging to Syndiniales (Alveolata). Environ. Microbiol. *10*, 3349–3365. https://doi.org/10.1111/j.1462-2920.2008.01731.x.
21. Sloboda, M., Kamler, M., Bulantová, J., Votýpka, J., and Modrý, D. (2008). Rodents as intermediate hosts of Hepatozoon ayorgbor (Apicomplexa: Adeleina: Hepatozoidae) from the African ball python, Python regius? Folia Parasitol. (Praha) *55*, 13–16. https://doi.org/10.14411/fp.2008.003.
22. Hartikainen, H., Stentiford, G.D., Bateman, K.S., Berney, C., Feist, S.W., Longshaw, M., Okamura, B., Stone, D., Ward, G., Wood, C., and Bass, D. (2014). Mikrocytids Are a Broadly Distributed and Divergent Radiation of Parasites in Aquatic Invertebrates. Curr. Biol. *24*, 807–812. https://doi.org/10.1016/j.cub.2014.02.033.
23. Kirk, N.L., Ritson-Williams, R., Coffroth, M.A., Miller, M.W., Fogarty, N.D., and Santos, S.R. (2013). Tracking Transmission of Apicomplexan Symbionts in Diverse Caribbean Corals. PLoS One *8*, e80618. https://doi.org/10.1371/journal.pone.0080618.
24. Toller, W., Rowan, R., and Knowlton, N. (2002). Genetic evidence for a protozoan (phylum Apicomplexa) associated with corals of the Montastraea annularis species complex. Coral Reefs *21*, 143–146. https://doi.org/10.1007/s00338-002-0220-2.
25. Amann, R.I., Binder, B.J., Olson, R.J., Chisholm, S.W., Devereux, R., and Stahl, D.A. (1990). Combination of 16S rRNA-targeted oligonucleotide probes with flow cytometry for analyzing mixed microbial populations. Appl. Environ. Microbiol. *56*, 1919–1925. https://doi.org/10.1128/aem.56.6.1919-1925.1990.
26. Keeling, P.J. (2002). Molecular phylogenetic position of Trichomitopsis termopsidis (Parabasalia) and evidence for the Trichomitopsiinae. Eur. J. Protistol. *38*, 279–286. https://doi.org/10.1078/0932-4739-00874.
27. Comeau, A.M., Li, W.K.W., Tremblay, J.É., Carmack, E.C., and Lovejoy, C. (2011). Arctic Ocean Microbial Community Structure before and after the 2007 Record Sea Ice Minimum. PLoS One *6*, e27492. https://doi.org/10.1371/journal.pone.0027492.
28. Bower, S.M., Carnegie, R.B., Goh, B., Jones, S.R., Lowe, G.J., and Mak, M.W. (2004). Preferential PCR Amplification of Parasitic Protistan Small Subunit rDNA from Metazoan Tissues. J. Eukaryot. Microbiol. *51*, 325–332. https://doi.org/10.1111/j.1550-7408.2004.tb00574.x.
29. Walters, W., Hyde, E.R., Berg-Lyons, D., Ackermann, G., Humphrey, G., Parada, A., Gilbert, J.A., Jansson, J.K., Caporaso, J.G., Fuhrman, J.A., et al. (2016). Improved Bacterial 16S rRNA Gene (V4 and V4-5) and Fungal Internal Transcribed Spacer Marker Gene Primers for Microbial Community Surveys. mSystems *1*, e00009-15. https://doi.org/10.1128/msystems.00009-15.
30. Geneious Prime (2023). Geneious Prime. Version 2023.0.4 (Dotmatics).
31. Katoh, K., and Standley, D.M. (2013). MAFFT Multiple Sequence Alignment Software Version 7: Improvements in Performance and Usability. Mol. Biol. Evol. *30*, 772–780. https://doi.org/10.1093/molbev/mst010.
32. Capella-Gutiérrez, S., Silla-Martínez, J.M., and Gabaldón, T. (2009). trimAl: a tool for automated alignment trimming in large-scale phylogenetic analyses. Bioinformatics *25*, 1972–1973. https://doi.org/10.1093/bioinformatics/btp348.

33. Nguyen, L.-T., Schmidt, H.A., von Haeseler, A., and Minh, B.Q. (2015). IQ-TREE: A Fast and Effective Stochastic Algorithm for Estimating Maximum-Likelihood Phylogenies. Mol. Biol. Evol. *32*, 268–274. https://doi.org/10.1093/molbev/msu300.

34. Martin, M. (2011). Cutadapt removes adapter sequences from high-throughput sequencing reads. EMBnet. j. *17*, 10–12. https://doi.org/10.14806/ej.17.1.200.

35. R Core Team (2023). R: A Language and Environment for Statistical Computing (Foundation for Statistical Computing).

36. Callahan, B.J., McMurdie, P.J., Rosen, M.J., Han, A.W., Johnson, A.J.A., and Holmes, S.P. (2016). DADA2: High-resolution sample inference from Illumina amplicon data. Nat. Methods *13*, 581–583. https://doi.org/10.1038/nmeth.3869.

37. McMurdie, P.J., and Holmes, S. (2013). phyloseq: An R Package for Reproducible Interactive Analysis and Graphics of Microbiome Census Data. PLoS One *8*, e61217. https://doi.org/10.1371/journal.pone.0061217.

38. Wickham, H., Averick, M., Bryan, J., Chang, W., McGowan, L., François, R., Grolemund, G., Hayes, A., Henry, L., Hester, J., et al. (2019). Welcome to the Tidyverse. J. Open Source Softw. *4*, 1686. https://doi.org/10.21105/joss.01686.

39. Paradis, E., and Schliep, K. (2019). ape 5.0: an environment for modern phylogenetics and evolutionary analyses in R. Bioinformatics *35*, 526–528. https://doi.org/10.1093/bioinformatics/bty633.

40. Yu, G., Smith, D.K., Zhu, H., Guan, Y., and Lam, T.T.-Y. (2017). ggtree: an r package for visualization and annotation of phylogenetic trees with their covariates and other associated data. Methods Ecol. Evol. *8*, 28–36. https://doi.org/10.1111/2041-210X.12628.

41. Xu, S., Dai, Z., Guo, P., Fu, X., Liu, S., Zhou, L., Tang, W., Feng, T., Chen, M., Zhan, L., et al. (2021). ggtreeExtra: Compact Visualization of Richly Annotated Phylogenetic Data. Mol. Biol. Evol. *38*, 4039–4042. https://doi.org/10.1093/molbev/msab166.

42. Lartillot, N., Rodrigue, N., Stubbs, D., and Richer, J. (2013). PhyloBayes MPI: phylogenetic reconstruction with infinite mixtures of profiles in a parallel environment. Syst. Biol. *62*, 611–615. https://doi.org/10.1093/sysbio/syt022.

43. Wang, Q., Garrity, G.M., Tiedje, J.M., and Cole, J.R. (2007). Naïve Bayesian Classifier for Rapid Assignment of rRNA Sequences into the New Bacterial Taxonomy. Appl. Environ. Microbiol. *73*, 5261–5267. https://doi.org/10.1128/AEM.00062-07.

44. Guillou, L., Bachar, D., Audic, S., Bass, D., Berney, C., Bittner, L., Boutte, C., Burgaud, G., de Vargas, C., Decelle, J., et al. (2013). The Protist Ribosomal Reference database (PR2): a catalog of unicellular eukaryote Small Sub-Unit rRNA sequences with curated taxonomy. Nucleic Acids Res. *41*, D597–D604. https://doi.org/10.1093/nar/gks1160.

45. Kalyaanamoorthy, S., Minh, B.Q., Wong, T.K.F., von Haeseler, A., and Jermiin, L.S. (2017). ModelFinder: fast model selection for accurate phylogenetic estimates. Nat. Methods *14*, 587–589. https://doi.org/10.1038/nmeth.4285.

46. Tabei, Y., Kiryu, H., Kin, T., and Asai, K. (2008). A fast structural multiple alignment method for long RNA sequences. BMC Bioinf. *9*, 33. https://doi.org/10.1186/1471-2105-9-33.

47. McGinnis, S., and Madden, T.L. (2004). BLAST: at the core of a powerful and diverse set of sequence analysis tools. Nucleic Acids Res. *32*, W20–W25. https://doi.org/10.1093/nar/gkh435.

STAR★METHODS

KEY RESOURCES TABLE

REAGENT or RESOURCE	SOURCE	IDENTIFIER
Chemicals, peptides, and recombinant proteins		
Ethyl Alcohol Anhydrous, USP (for sample fixation prior to DNA extraction)	Commercial Alcohols	Item#P006EAAN
Phusion High-Fidelity PCR Master Mix with HF Buffer (for PCR)	ThermoFisher Scientific	Cat#F531L
UltraPure DNase/RNase-free distilled water (for PCR)	ThermoFisher Scientific	Cat#10977023
para-formaldehyde	Electron Microscopy Sciences	Cat#15700
DAPI	ThermoFisher Scientific	Cat#62248
Coarse Sea Salts	Gathering Place	N/A
6X GelRed® Prestain Loading Buffer with Orange Tracking Dye	Biotium	Cat#41010
Critical commercial assays		
DNeasy PowerBiofilm Kit	QIAGEN	Cat. No./ID: 24000-5
Monarch DNA Gel Extraction Kit	New England Biolabs	Cat#T1020S
QIAquick PCR Purification Kit	QIAGEN	Cat#28104
Qubit™ 1X dsDNA High Sensitivity (HS) Assay Kit	ThermoFisher Scientific	Cat#Q33230
Deposited data		
Microbiome SSU raw reads	This paper	BioProject number PRJNA1048503
SSU gene sequences	This paper	GenBank OR883650-OR883663
Oligonucleotides		
5′-CTGTCAAGAACAAGCGGTCC-3′	This paper	18N_F_WK
5′-CTTAGAACCAATAAAATAGAACTGAAA-3′	This paper	18N_R_WK
5′-ACAGTTATAGTTTATTTGATGGCT-3′	This paper	CCH_F
5′-CAGGAACAAGGGTTCCCGACC-3′	Toller et al.[24]	18N-R1
5′-GTYCTTAGAACCAATAAAATAGAACTG-3′	This paper	18N_R_WK_exA
5′-CAGCAAGGTTCAGAAGAAAG-3′	This paper	R-coralFront
5′-CCAGTTTCCTTCAGCACCTTATGA-3′	This paper	F-coralEnd
5′-GTGTGTCTAACACAAGGAAGTTTG-3′	This paper	More_F1
5′-Fluorescein-GCTGCCTCCCGTAGGAGT-3′	Amann et al.[25]	EUB338
5′-TexasRedX-CTGCGCATATAAGGAATTAC-3′	Kwong et al.[5]	WK16
5′- Fluor532-TCAGAAGAAAGTCAAAAACG-3′	Kwong et al.[5]	WK17
5′-TGATCCTTCTGCAGGTTCACCTAC-3′	Keeling[26]	FAD4
5′-CYGCGGTAATTCCAGCTC-3′	Comeau et al.[27]	E572F
5′-AYGGTATCTRATCRTCTTYG-3′	Comeau et al.[27]	E1009R
5′-GTGCCAGCAGCCGCG-3′	Bower et al.[28]	UnonMetaF
5′-TTTAAGTTTCAGCCTTGCG-3′	Bower et al.[28]	UnonMetaR
5″- GTGYCAGCMGCCGCGGTAA-3″	Walters et al.[29]	515FB
5″- GGACTACNVGGGTWTCTAAT-3″	Walters et al.[29]	806RB
Software and algorithms		
Geneious Prime *De novo* assembler	Geneious Prime 2023.0.4[30]	N/A
MAFFT v. 7.481	Katoh and Standley[31]	N/A
trimAl 1.2rev59	Capella-Gutierrez et al.[32]	N/A
IQ-TREE 1.6.12	Nguyen et al.[33]	N/A
cutadapt v.3.4.	Martin[34]	N/A
R v.4.3.	R Core Team[35]	N/A
DADA2 v.1.28.0.	Callahan et al.[36]	N/A
phyloseq v.1.44.0.	McMurdie and Holmes[37]	N/A

(*Continued on next page*)

Continued

REAGENT or RESOURCE	SOURCE	IDENTIFIER
tidyverse v.2.0.0.	Wickham et al.[38]	N/A
ape v.5.7.1.	Paradis and Schliep[39]	N/A
ggTree v.3.8.2.	Yu et al.[40]	N/A
ggTreeExtra v.1.10.0	Xu et al.[41]	N/A
PhyloBayes-MPI (v.4.0.3)	Lartillot et al.[42]	N/A

RESOURCES AVAILABILITY

Lead contact

Requests for further information, resources, and reagents can be directed to the lead contact Patrick Keeling (pkeeling@mail.ubc.ca).

Materials availability

This study did not generate new unique reagents.

Data and code availability

- New 18S SSU genes characterized in this study have been deposited to GenBank and are publicly available as of the date of publication. Accession numbers are listed in the key resources table. Microbiome raw reads from anthozoan hosts have been deposited in the NCBI Short Read Archive (SRA) under BioProject number PRJNA1048503, publicly available as of the date of publication.
- This paper does not report any original code.
- Any additional information required to reanalyze the data reported in this paper is available from the lead contact upon request.

EXPERIMENTAL MODEL AND STUDY PARTICIPANT DETAILS

Samples were collected at five locations along the coast of British Columbia, Canada, and one site in Curaçao (Table S1). The anthozoans were collected by carefully removing them from the substrate to minimize stress and stored in seawater with bubblers while in transit to the laboratory. For a subset of samples, anthozoans were dissected by tissue type (mesenterial filaments, tentacles, dermis, acontia), otherwise the whole polyp was dissected, fixed in 100% ethanol, and stored at room temperature until DNA extraction. DNA extraction was then conducted according to the DNeasy PowerBiofilm Kit protocol, and DNA concentration (ng/μL) was measured using the Qubit 1X dsDNA High Sensitivity (HS) Assay Kit.

METHOD DETAILS

Screening of corallicolid infection

To determine whether sampled anthozoans were positively infected, corallicolid specific primers were designed (18N_F_wk, 18N_R_wk) from cold-water corallicolid amplicon reads that target the V4 region of the 18S rRNA gene obtained from Illumina short-read amplicon sequencing. PCR reactions and thermocycling conditions were conducted using the standard Phusion High-Fidelity PCR Master Mix with HF Buffer protocol (New England BioLabs), modified for a 40 μL reaction: 2 μL of 10 μM Forward Primer, 2 μL Reverse Primer, 20 μL 2X Phusion Master Mix, 12 μL Nuclease-free water, and 12 μL Template DNA. When possible, DNA was diluted to achieve a concentration of 25 ng/μL. UltraPure Distilled Water (Invitrogen) was used as a negative control. PCR products were mixed with 6X GelRed Prestain Loading Buffer with Orange Tracking Dye (Biotium) as per product instruction and visualized (expected band size ~212 bp) using gel electrophoresis with 1% agarose gels.

Microbiome sequencing and phylogenetic analysis

Libraries for eukaryotic microbiome amplicon sequencing were prepared using metazoan-excluding primers which targeted the V4 region of the 18S rRNA gene (UnonMetaF, UnonMetaR).[28] The resulting product was dyed with 6X GelRed Prestain Loading Buffer with Orange Tracking Dye and visually inspected using gel electrophoresis to ensure successful amplification; cleaned with QIAquick PCR Purification Kit; and quantified using the QubitTM 1X dsDNA High Sensitivity Assay Kit. Samples with satisfactory yield were sent to the Integrated Microbiome Resource (IMR) facility at Dalhousie University in Nova Scotia, Canada for sequencing on the Illumina MiSeq sequencing, using a nested eukaryotic-specific primer set targeting the V4 region (E572F, E1009R).[27]

Libraries for bacterial microbiome sequencing were prepared and sequenced at IMR facility according to their standardized protocol (https://imr.bio/protocols.html). Extracted DNA from anemone tissues were first diluted using 1:1 and 1:10 ratios and amplicon

libraries were prepared using prokaryotic-specific "fusion primers" (containing Illumina adaptors and indices) that target the V4 region of the 16S rRNA gene (515FB, 806RB).[29] PCR products from pooled dilutions were then cleaned using the Charm Biotech Just-a-Plate 96-well Normalization Kit before sequencing on an Illumina Miseq using 300bp reads.

PCR primer and sequencing adapter sequences were removed from raw sequencing reads using Cutadapt (v.3.4.)[34] and processed in R (v.4.3.)[35] following the DADA2 pipeline (v.1.28.).[36] In brief, reads were filtered and trimmed using standard filtering parameters (maxN = 0, maxEE = c(2,2), truncQ = 2) before generating run-specific error models for both forward and reverse reads to estimate their respective error rates. The DADA2 sample inference algorithm was run with "pseudo" pooling to increase sensitivity to low frequency sequence variants present in multiple samples. Chimeras were removed from merged reads using the "consensus" method before assigning taxonomy using the naive Bayesian classifier[43] and the PR2 database.[44] The final OTU table was combined with PR2 taxonomic assignments and sample metadata using the phyloseq package (v.1.44.0).[37]

Corallicolid sequences over 0.001 relative abundance (> 0.1%) were identified by aligning ASVs assigned as apicomplexans against full-length reference sequences using the EINS-I MAFFT (v. 7.48)[31] alignment algorithm. A Maximum Likelihood (ML) phylogeny was inferred with IQ-TREE (v.1.6.12)[33] using Model Finder[45] to choose the optimum substitution model. Sequence variants clustering outside of the corallicolid clade were discarded.

To compare anemone ASVs with those from coral, published eukaryotic sequencing surveys of coral microbiomes were identified on GenBank. Data from 12 studies were obtained (Table S2) and processed as above, combining all datasets after independent processing with the DADA2 pipeline. All ASVs above 0.01% in at least one sample and assigned to the family Corallicolidae were extracted, resulting in the inclusion of four studies. Including ASVs assigned to the Order Eimeriida did not reveal additional corallicolid sequences (determined phylogenetically).

A final ML phylogeny with corallicolid ASVs from both anemones and coral was generated as above but using the MAFFT-XINSI algorithm, which uses MXSCARNA to assess secondary structure information.[46] The resulting tree file was imported to R using the phyloseq package[37] and re-rooted using the ape package (v.5.7.1.).[39] A cladogram was plotted using the ggTree (v.3.8.2.)[40] and ggTreeExtra (v.1.10.0.)[41] packages, adding accompanying host information as additional layers.

To visualize entire microbiomes, eukaryotic and prokaryotic ASVs were independently agglomerated to the Class and Order level (respectively), their read counts transformed to relative abundance, and filtered to only include those greater than 0.1% relative abundance in at least one sample. Only samples with more than 1000 reads were included. The resulting dataset was plotted as a heatmap using the ggplot2 package[38] where fill color scales to abundance values.

Full-length SSU sequencing and phylogenetic analysis

Primer sets used previously to amplify the SSU of coral-infecting corallicolids[5] resulted in the amplification of Actiniaria and other non-coral Anthozoa hosts, therefore, a series of primer sets were developed and tested: CCH_F,18N_R_wkexA; 18N_F_wk, FAD4[26]; and More_F1, FAD4 were used to amplify the majority of *M. senile*, and both *Edwardsiella* sp. The aforementioned primer sets were less successful in obtaining long and high-quality fragments from *C. californicus.* Thus, R-coralFront and F-coralEnd were designed, and used along with 18N-R1 (CCH_F, R-coralFront; F-coralEND, FAD4; 18N_F_wk, 18N-R1[24]) to fill in gaps of the *C. californicus* SSU sequence. PCR reactions and thermocycling conditions were conducted using the Phusion High-Fidelity PCR Master Mix with HF Buffer following the manufacturer's protocol. UltraPure Distilled water was used as a negative control and samples previously confirmed to contain corallicolids were used as a positive control. PCR products were visualized via gel electrophoresis as above and purified using the Monarch DNA Gel Extraction Kit (New England Biolabs) before quantification. Products with sufficiently high yield were sent to the Sequencing + Bioinformatics Consortium at the University of British Columbia in BC, Canada for Sanger dideoxy sequencing using the Applied Biosystems 3730S 48-capillary DNA Analyzer and BigDye Terminator v3.1 Sequencing Chemistry.

Sequence chromatograms were inspected, and low-quality ends were trimmed manually using Geneious Prime.[30] The identity of trimmed sequences was confirmed via BLASTn[47] searches of the NCBI megaBLAST nucleotide database. Fragments of the same host individual were then assembled using Geneious Prime *de novo* assembler. Assembled sequences with a minimum HQ of 85% (as defined by the default setting of Geneious Prime), and publicly available corallicolid sequences (Table S3) were filtered to select only those longer than 800bp, with the exception of two sequences generated in this study (659bp and 707bp), to be used for phylogenetic analysis. An alignment was then constructed with nine additional Apicomplexa sequences as the outgroup with MAFFT v. 7.481[31] using the MAFFT-XINSI algorithm. The alignment was then visually inspected with Geneious Prime, and miss-alignments were manually corrected. In cases of identical sequences isolated from both the same host species and location, the shorter sequence(s) was removed before being trimmed with trimAl 1.2rev59[32] using a gap threshold of 0.4 and a similarity threshold of 0.001. The sequence MH304759 was divergent and removed. The trimmed alignment, containing 1582 positions, was then used to conduct a ML analysis using IQ-TREE 1.6.12.[33] The ModelFinder[45] feature was used to find the best-fit model as determined by IQ-TREE (TN + F + R2). To corroborate the resulting tree, PhyloBayes-MPI (v.4.0.3) was used to perform a Bayesian analysis on the same alignment using four parallel chains and the CAT+GTR+G4 model.[42] A consensus tree (Figure S3A) was built after approximately 29,000 trees in each chain and reported a maxdiff value of 0.03.

As supplemental information two additional ML tree were also constructed. Both trees used the same parameters stated above, with the inclusion of all sequences over 659bp, and all identical sequences from the same host species and location were included in the subsequent alignment and ML analysis (Figure S3B); the second also contains the divergent sequence MH304759 (Figure S3C).

The ModelFinder feature was once again used to find the best-fit model as determined by IQ-TREE (HKY+F+R2 for both). For all ML iterations (including Figure 3) 1000 non-parametric bootstrap pseudoreplicates were performed.

Fluorescence *in situ* hybridization (FISH)

M. *senile* and C. *californicus* from Quadra Island, British Columbia were transported to UBC and maintained in a benchtop aquarium for several days (M. *senile*) or several weeks (C. *californicus*). Individuals selected for FISH were co-sampled for 18S identification and screened positive for corallicolids using 18N_F_WK and 18N_R_WK as PCR primers. 13 individuals of C. *californicus* were dissected in the sagittal plane to generate tissue sections that contained tentacles, body wall, and mesenterial filaments. Mesenterial filaments from 20 M *senile* individuals were isolated with forceps into small tissue clumps (< 1 cm3). Tissues from both species were fixed with 4% paraformaldehyde in 0.6 M sea salts for 1 h at room temperature. Tissue sections were rinsed with sea salts and dehydrated in a graded ascending ethanol series (30%, 50%, 70%, 95%, 100% x3) for 15 min at each step. Tissues were cleared in 6% H_2O_2 and 70% EtOH (v/v) for 72 h on a rotary shaker (80 RPM) at room temperature. Samples were rehydrated in aqueous wash buffer (WB) containing 50 mM Tris-HCl and 900 mM NaCl for 15 min x2. Non-specific binding of fluorescent probes to nematocysts were quenched by incubating tissue sections with 0.1 μM EUB338-Fluorescein bacterial probe[24] in hybridization buffer (WB + 0.1% v/v sodium dodecyl sulfate) for 3 h at 46 C in a dark humidity chamber. Samples were then washed twice for 10 min in a probe-free hybridization buffer. Tissues were hybridized with 0.1 μM corallicolid-specific probes (WK16 and WK17[5] in hybridization buffer for 12 h at 46°C in a dark humidity chamber. After washing the tissues with probe-free hybridization buffer and subsequently dH2O, tissues were counterstained with 1 μM DAPI for 10 min at room temperature. Tissue sections were mounted in citifluor mounting solution with a #1.5 coverslip and sealed with paraffin wax.

Bright field and fluorescence imaging was performed with an Olympus BX53 microscope equipped with an Olympus DP80 digital camera and CellSense Standard software (Olympus). Standard filter sets for DAPI, eGFP (EUB338), TRITC (ARL-V 16S probe), and Cy5 (type-N 18S probe) were used to collect the fluorescence emission from each probe respectively. Image acquisition parameters (i.e., laser intensity and exposure time) were optimized for each objective lens to maximize the signal-to-noise ratio, then kept constant for the remainder of the imaging session.